

DOUBLE-PEAKED BROAD LINE EMISSION FROM THE LINER NUCLEUS OF NGC 1097

THAISA STORCHI-BERGMANN¹

Departamento de Astronomia, IF-UFRGS, CP 15051, CEP 91501-970, Porto Alegre, RS, Brazil

JACK A. BALDWIN

Cerro Tololo Inter-American Observatory, National Optical Astronomy Observatories, Casilla 603, La Serena, Chile

AND

ANDREW S. WILSON¹

Space Telescope Science Institute, 3700 San Martin Drive, Baltimore, MD 21218, and Astronomy Department, University of Maryland, College Park, MD 20742

Received 1993 January 19; accepted 1993 March 22

ABSTRACT

We report the recent appearance of a very broad component in the H α and H β emission lines of the weakly active nucleus of the Sersic-Pastoriza galaxy NGC 1097. Subtraction of the contribution of the stellar population from our spectra reveals that the FWZI of the broad component is about 21,000 km s⁻¹ and that its profile is double-peaked. The data also suggest the presence of a blue, featureless continuum in the nucleus. The H α /H β flux ratio indicates that the broad-line region (BLR) is not significantly reddened. The broad component was first observed in H α in 1991 November 2, and confirmed 11 months later. The H α profile and flux did not change in this time interval. Comparison with previously published spectral data indicates that the broad lines have only recently appeared. Together with the relatively high X-ray luminosity and the compact nuclear radio source, our results characterize the presence of a Seyfert 1 nucleus in a galaxy which had previously shown only LINER characteristics. The simplest interpretation is that obscuring material along our line of sight to the nucleus has recently cleared, permitting a direct view of the active nucleus. We discuss two possible structures for the broad line region—biconical outflow and an accretion disk—that could give rise to the observed profile. We also speculate on the relationship between the broad line region and the previously known optical jets, which extend to tens of kpc from the nucleus.

Subject headings: galaxies: individual (NGC 1097) — galaxies: jets — galaxies: nuclei — galaxies: Seyfert — line: profiles

1. INTRODUCTION

NGC 1097 is a southern barred spiral galaxy which has been extensively studied from X-rays to radio wavelengths. Optical observations show an active nucleus previously classified as a LINER (Keel 1983; Phillips et al. 1984), surrounded by a 1.5 kpc (for $H_0 = 75$ km s⁻¹ Mpc⁻¹) diameter ring of H II regions and hot spots (Burbidge & Burbidge 1960; Sersic & Pastoriza 1965; Phillips et al. 1984, and references therein). Forbes et al. (1992) present recent images of NGC 1097 in the *B* band and near-infrared, which show that the ring is actually a tightly wound spiral. But the most remarkable feature in the optical is the presence of four faint jets, discovered by Wolstencroft & Zealey (1975), Arp (1976), and Lorre (1978), extending to about 90 kpc and directed radially from the nucleus.

In the radio, VLA observations show that the emission is dominated by the star-forming ring, but coincident with the nucleus there is a compact (less than 8 pc) source with an inverted radio spectrum indicative of synchrotron self-absorption (Hummel, van der Hulst, & Keel 1987; Wolstencroft, Perley, & Tully 1984). NGC 1097 is also a relatively strong X-ray source, with $L_x = 1.1 \times 10^{41}$ ergs s⁻¹ (Fabbiano, Kim, & Trinchieri 1992).

As part of an ongoing project to study the dynamics and

chemical abundance of star-forming regions in the neighborhood of active galactic nuclei (AGNs), we have obtained several long-slit spectra of the nuclear region of NGC 1097. In this *Letter*, we present and discuss the spectra of the active nucleus, which have unexpectedly shown strong broad components in the Balmer lines, not observed in previous studies.

2. OBSERVATIONS

The observations were made at two epochs 11 months apart, using CCD detectors on the Cassegrain Spectrograph at the CTIO 4 m telescope. On 1991 November 2, the spectral range covered was 6200–7070 Å, with a spectral resolution of 1.7 Å. A GG495 filter was used to block possible higher grating order contamination. The nuclear spectrum was obtained under photometric conditions in four different long-slit exposures of 900 seconds each, taken through a 2" slit. Two exposures were made at position angle (p.a.) 130° and two at p.a. 40°. We will refer to these observations as the high-resolution spectra in the rest of the paper.

Another long-slit spectrum of the nucleus was kindly obtained for us by J. Maza on 1992 October 5. The telescope, spectrograph and slit width were the same as for the previous observations, but the spectral range was 3200–7100 Å, with 8 Å resolution. The nuclear spectrum was obtained in an exposure of 685 seconds, with the slit at p.a. 130°, under nonphotometric conditions. We will call this observation the low-resolution spectrum.

¹ Visiting Astronomer at the Cerro Tololo Inter-American Observatory, operated by the Association of Universities for Research in Astronomy, Inc., under contract with the National Science Foundation.

The spectra were reduced using the IRAF software, including flux calibration through observations of standard stars. Since the low-resolution spectrum was taken through clouds, it was normalized to the high-resolution ones by forcing the flux levels in the stellar continuum (after binning a $6''$ length along the slit) to be the same. We verified that the required scaling factor also gives good agreement between the narrow emission line fluxes in the two spectra.

3. RESULTS

3.1. Broad Emission Lines

The high-resolution nuclear spectrum from the combined observations with the slit in p.a. 130° is shown in Figure 1, where a very broad $H\alpha$ line can readily be seen, with the narrow $H\alpha$ component and the $[N\ II] \lambda\lambda 6548, 6583$ lines on top of it. The $[S\ II] \lambda\lambda 6717, 6731$ lines also appear superposed on the red wing of the broad $H\alpha$ emission. An identical $H\alpha$ profile is obtained from the spectra in p.a. 40° . The low-resolution nuclear spectrum is shown in Figure 2. It can be seen that the broad $H\alpha$ component is still present, almost 1 year after the high-resolution spectra were taken. It can further be seen that a broad component is also present in $H\beta$, with its red wing blended with the $[O\ III] \lambda 4959$ emission line. No narrow $H\beta$ component is seen. The broad profiles are not resolved spatially along the slit; we determined this by subtracting the spatial profile of the galaxy (measured in the nearby continuum) from the $H\alpha$ spatial profile, and found that the

resulting difference profile along the slit was indistinguishable from that of a star measured on the same night.

3.2. Correction for Underlying Stellar Population

In the (uppermost) spectra of Figures 1 and 2, many absorption features due to the stellar population can be identified. In order to better isolate the emission lines, it is necessary to subtract the underlying stellar contribution. We have chosen the extracted spectra $3''.6$ NW of the nucleus along p.a. 130° as representative of the stellar population. These spectra were selected because they have good S/N ratios, are not contaminated by the broad $H\alpha$ emission, and show the same stellar population features as the nuclear spectra. These spectra were then corrected to the same velocity as that of the nuclear spectra by comparing the wavelengths of the narrow emission lines, assuming that the stellar and gaseous kinematics are similar. In order to eliminate the narrow $H\alpha$ and $[N\ II] \lambda\lambda 6548, 6583$ emission lines from the off-nuclear spectra, we have replaced the corresponding spectral region with that of a template population (Bica 1988) which shows similar stellar spectral features. We then scaled the results to the flux of the nuclear spectrum in spectral regions far from the broad lines. The final, adopted spectra of the stellar population are shown as the middle spectra in Figures 1 and 2 (shifted in flux for clarity). We then subtracted them from the corresponding nuclear spectra to obtain the emission spectra shown at the bottom of the figures.

Figure 1 demonstrates the excellent match between the stellar population features in the nucleus and those $3''.6$ NW of the nucleus over the limited range covered by the high-resolution spectrum. For the low-resolution spectrum (Fig. 2), where the S/N ratio is lower and the spectral range larger, the match of the population is not as good for $\lambda < 6200 \text{ \AA}$. However, the agreement is still better than 10% of the continuum value for $\lambda > 4000 \text{ \AA}$. The much larger differences for $\lambda < 4000 \text{ \AA}$ will be discussed below.

3.3. Line Profiles, Fluxes, and Reddenings

The high S/N ratio of the high-resolution spectra permits a very good definition of the broad $H\alpha$ profile (*bottom spectrum*, Fig. 1). The profile shows an impressive double-peaked structure, with the stronger peak redshifted relative to the narrow $H\alpha$ component and the other one blueshifted. The velocity measured for the central wavelength of the narrow $H\alpha$ component agrees with that adopted for the systemic velocity. Relative to this velocity, the blue and red peaks are shifted by, respectively, $V = -3300 (\pm 100) \text{ km s}^{-1}$ and $V = 3950 (\pm 100) \text{ km s}^{-1}$. The blue wing is more extended than the red wing, corresponding to a relative velocity at the bluest wavelength of $V = -12,800 (\pm 500) \text{ km s}^{-1}$, while the reddest wavelength corresponds to $V = 8500 (\pm 200) \text{ km s}^{-1}$. The FWZI is thus about $\Delta V = 21,000 \text{ km s}^{-1}$. Analysis of the low-resolution spectrum after subtraction of the stellar population (*bottom spectrum*, Fig. 2) shows good agreement between the broad $H\alpha$ and $H\beta$ profiles (after subtracting the superposed narrow lines and rebinning to velocity space).

We have used spectral extractions with a $6''$ window along the slit to compare the $H\alpha$ profiles in the high- and low-resolution spectra, after subtraction of the stellar population contribution. The two profiles are shown in Figure 3. The differences between the narrow line profiles are due to the different resolution of the two spectra. There is no significant difference between the broad $H\alpha$ profile in the two observa-

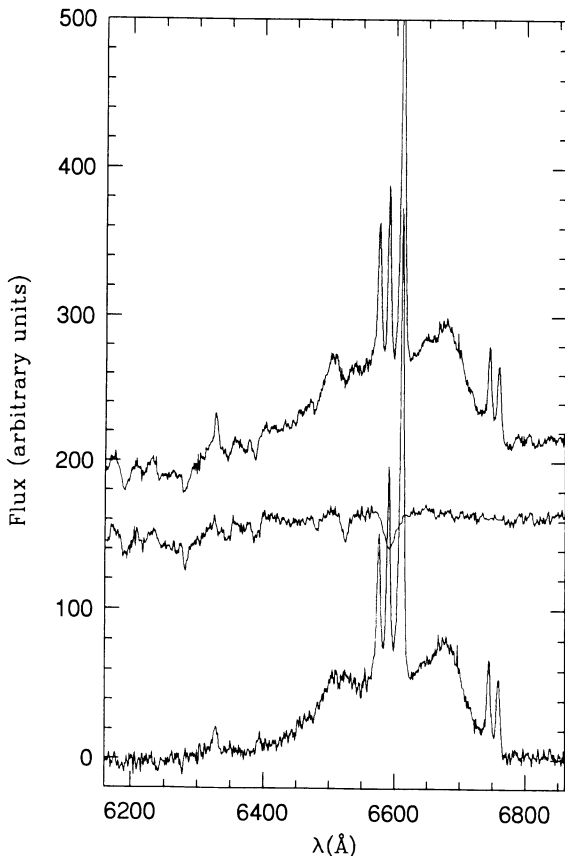


FIG. 1.—Observed nuclear high-dispersion spectrum (*top*), adopted stellar population spectrum (*middle*), and the difference observed spectrum minus stellar population (*bottom*). Two pixels along the slit were binned together, giving an effective aperture of $2'' \times 1''.8$ (167×150 pc).

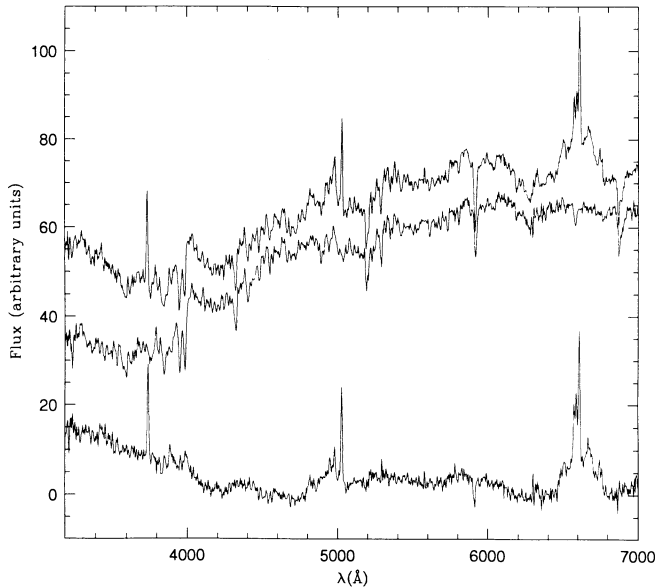


FIG. 2.—Observed nuclear low-dispersion spectrum (*top*), adopted stellar population spectrum (*middle*) and the difference observed spectrum minus stellar population (*bottom*). The effective aperture is the same as in Fig. 1.

tions. This result is confirmed by a comparison of the emission line fluxes: the $H\alpha$ broad line fluxes in the two spectra agree to within 10%, which is similar to the agreement between the narrow line fluxes. We thus conclude that the broad line profile has not change during the 11 month interval between the two observations.

The emission line fluxes obtained from the 6" window spectra are listed in Table 1. It is interesting to compare the Balmer decrements obtained from the narrow and broad lines: $(H\alpha/H\beta)_{\text{narrow}} \geq 6.8$ (as obtained from the upper limit to the

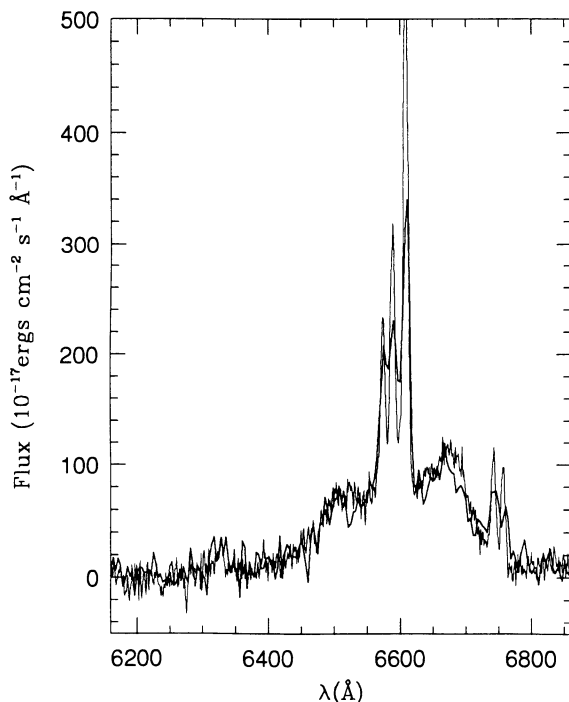


FIG. 3.—Comparison between the high-dispersion profile and the low-dispersion profile, obtained 11 months later.

TABLE 1
EMISSION-LINE FLUXES

Line (λ_{lab})	Flux (10^{-15} ergs cm^{-2} s^{-1})
[O II] $\lambda 3727$	17.3
$H\beta_{\text{narrow}}$	< 3
$H\beta_{\text{broad}}$	64.1 (± 8)
[O III] $\lambda 4958.9$	5.5
[O III] $\lambda 5006.9$	18.4
[O I] $\lambda 6300.3$	2.4
[O I] $\lambda 6363.8$	0.7
[N II] $\lambda 6548.1$	13.3
$H\alpha_{\text{narrow}}$	21.0
$H\alpha_{\text{broad}}$	219.1 (± 10)
[N II] $\lambda 6583.4$	44.0
[S II] $\lambda 6716.4$	7.6
[S II] $\lambda 6730.8$	7.3

$H\beta$ flux), while $(H\alpha/H\beta)_{\text{broad}} = 3.2 \pm 0.5$. This indicates that, although the NLR is significantly reddened [$E(B-V) \geq 0.73$], the BLR has practically no reddening at all. We are thus probably observing the broad line region, and perhaps the nuclear nonstellar continuum (see below) through a “clearing” in the narrow line region.

3.4. Excess Blue Continuum?

Figure 2 shows that the nuclear continuum for $\lambda < 4000 \text{ \AA}$ is significantly bluer than a stellar population which matches the spectrum for larger λ 's. There is an increasing excess of the nuclear continuum over the stellar population contribution as λ decreases, reaching a value of 50% above the population continuum at 3300 \AA . The low-resolution observation shown in Figure 2 was taken when NGC 1097 was less than 1 degree from the zenith, so the energy distribution should be reliable in spite of the narrow slit and wide wavelength range.

The nuclear continuum could be bluer than the 3"6 NW spectrum because of a smaller reddening. If this were the case, and the stellar population is the same, the equivalent widths of the absorption lines should be the same. To check this, we measured the equivalent widths of the Ca II K and H lines (windows $3908\text{--}3952 \text{ \AA}$ and $3952\text{--}3988 \text{ \AA}$, the G-band ($4284\text{--}4318 \text{ \AA}$) and the MgI + MgH ($5156\text{--}5196 \text{ \AA}$) feature. We found that, while the MgI + MgH and G-band absorption features have the same equivalent widths in the spectrum of the nucleus as in the 3"6 NW spectrum, the equivalent widths of the Ca II H and K lines are 30% smaller in the nucleus. This is a significant difference which therefore argues against reddening as the full explanation of the excess blue continuum. We also tried to deredden the 3"6 NW spectrum by different amounts and find that the reddening difference cannot be larger than $E(B-V) = 0.05$: for larger values, there is no match with the nuclear continuum shape for $\lambda > 4000 \text{ \AA}$.

We thus conclude that there is evidence for the presence of a lineless (or weak-lined) blue excess continuum in the nucleus.

4. DISCUSSION

4.1. Comparison with Previous Observations

The nuclear spectrum of NGC 1097 has been observed several times over the last decade. Our narrow line fluxes (Table 1) agree with those of Véron-Cetty & Véron (1986, hereafter VCV) to within 30%, and with those of Keel (1983) to within a factor of 2–3 in $H\alpha$, [N II] and [S II], and much better in [O III]. However, neither of these papers mentions the pres-

ence of a broad H α component. Inspection of Keel's spectra (taken in 1981 and 1983 and kindly provided by W. C. Keel and W. Zheng) and those shown in Phillips et al.'s (1984) Figures 1 and 3 (taken in 1981) shows no broad component. Although the S/N ratio of these spectra is lower than ours, the [S II] lines are clearly seen and we judge that the broad component of H α would have been detected if it were present at our observed flux level.

These results indicate that the broad component has appeared only recently. In this respect, NGC 1097 is similar to other low-luminosity active nuclei, like NGC 6814, which was observed with broad H α and H β emission lines by VCV, but later had no broad-line emission at all (Morris & Ward 1988; Winge et al. 1993). Another AGN showing similar behavior is NGC 1566 (Pastoriza & Gerola 1970; Alloin et al. 1986).

4.2. Models for Double-Peaked Profiles

Double-peaked, broad Balmer profiles can be produced in at least three distinct scenarios (cf. Eracleous & Halpern 1992): (1) the BLR is undergoing biconical outflow (e.g., as "jets"); (2) the broad Balmer lines originate in an accretion disk surrounding a supermassive black hole; (3) there are two separate BLRs (perhaps due to the presence of a binary black hole). We will discuss here only the first two possibilities, as a test of the third one would require monitoring of the velocities of the two peaks of the broad line emission, which has not yet been done.

Zheng, Binette, & Sulentic (1990), and Zheng, Veilleux, & Grandi (1991) have proposed a model in which the BLR has a biconical shape. Considering that NGC 1097 shows four optical jets that seem to emanate from the nucleus, it is reasonable to suppose that the broad-line emission could be due to gas recently ejected from the active nucleus in a biconical morphology. The above authors show that, depending on the luminosity distribution along the jets, a double-peaked profile can result and, if the physical conditions in each jet are not identical, one wing can be stronger than the other.

Double-peaked broad emission lines can also originate in accretion disks. Chen, Halpern, & Filippenko (1989) and Chen & Halpern (1989) have shown that the double-peaked broad H α profiles of Arp 102B and 3C 390.3 can be fitted by accretion disk models. Comparison of the broad H α profile of NGC 1097 with that of Arp 102B (e.g., Fig. 1 of Chen & Halpern 1989), shows a qualitative similarity. Nevertheless, a closer look at the NGC 1097 profile shows characteristics that cannot be reproduced by models similar to those for Arp 102B and 3C 390.3: whereas the model predicts a blue peak more intense

than the red one due to Doppler boosting and a red wing more extended than the blue, the NGC 1097 broad H α profile shows the opposite characteristics. One possibility under study is that the accretion disk is elliptical (Syer & Clarke 1992): such a disk could be possible if it was recently formed by disruption of stars, or if the galactic potential in the nucleus is not azimuthally symmetric. In this case, the red peak could be stronger than the blue and the blue wing more extended than the red (Halpern 1992), as observed.

4.3. Comparison with Seyfert 1's

The active nucleus of NGC 1097 now has several characteristics of a Seyfert 1 nucleus: it has broad Balmer lines with FWHM of about 10,000 km s⁻¹; there may be a featureless blue continuum; and the radio spectrum shows synchrotron self-absorption. NGC 1097 is also an X-ray emitter at the 10⁴¹ ergs s⁻¹ level, although the fraction of this emission associated with the active nucleus is uncertain. The broad H β and X-ray fluxes of NGC 1097 fit nicely on the correlation between these quantities found for Seyfert 1 galaxies (e.g., Kriss, Canizares, & Ricker 1980). If the X-ray emission is mostly nuclear, this result argues for a long-lived broad line region, for the X-ray measurements were made in 1979. We can then say that NGC 1097 harbors a mini-Seyfert 1 nucleus, as the H α luminosity is 7.7×10^{39} ergs s⁻¹, about three orders of magnitude smaller than that of the most luminous Seyfert 1's. The characteristics of NGC 1097 have become very similar to those of NGC 7213 (Filippenko & Halpern 1984), which also has broad H α emission and nonstellar continuum radiation (accounting for at least 50% of the observed continuum at $\lambda 3300$ Å), a flat-spectrum radio source, and a high X-ray/optical luminosity ratio (Halpern & Filippenko 1984).

The nuclear activity in NGC 1097 is presumably related to its remarkable optical jets. We may be seeing a new jet in formation: the broad lines could either originate from the double jet itself or be the signature of an accretion event in an elliptical disk that will give rise to another pair of jets in the future.

We thank Jules Halpern, Horacio Dottori, Sylvain Veilleux, Eduardo Bica, and Charles Bonatto for helpful discussions, as well as the referee, Wei Zheng, for valuable comments. We are indebted to Jose Maza for obtaining the low-dispersion spectrum. T. S. B. acknowledges the Brazilian institutions CNPq, CAPES and FAPERGS for partial support. A. S. W. thanks NASA for support under grants NAGW-2689 and NAG8-793.

REFERENCES

- Alloin, D., Pelat, D., Fosbury, R. A. E., Freeman, K., & Phillips, M. M. 1986, *ApJ*, 308, 23
 Arp, H. C. 1976, *ApJ*, 207, L147
 Bica, E. 1988, *A&A*, 195, 76
 Burbidge, E. M., & Burbidge, G. R. 1960, *ApJ*, 132, 30
 Chen, K., & Halpern, J. 1989, *ApJ*, 344, 115
 Chen, K., Halpern, J., & Filippenko, A. V. 1989, *ApJ*, 339, 742
 Eracleous, M., & Halpern, J. 1992, in *AIP Conf. Proc.* 254, Testing the AGN Paradigm, ed. S. S. Holt, S. G., Neff, & C. M. Urry (New York: AIP), 220
 Fabbiano, G., Kim, D.-W., & Trinchieri, G. 1992, *ApJS*, 80, 531
 Filippenko, A. V., & Halpern, J. P. 1984, *ApJ*, 285, 458
 Forbes, D. A., Ward, M. J., Depoy, D. L., Boisson, C., & Smith, M. S. 1992, *MNRAS*, 254, 509
 Halpern, J. 1992, private communication
 Halpern, J., & Filippenko, A. 1984, *ApJ*, 285, 475
 Hummel, E., van der Hulst, J. M., & Keel, W. C. 1987, *A&A*, 172, 32
 Keel, W. C. 1983, *ApJ*, 269, 466
 Kriss, G. A., Canizares, C. R., & Ricker, G. R. 1980, *ApJ*, 242, 492
 Lorre, J. J. 1978, *ApJ*, 222, L99
 Morris, S., & Ward, M. 1988, *MNRAS*, 230, 639
 Pastoriza, M. G., & Gerola, H. 1970, *Astrophys. Lett.*, 6, 155
 Phillips, M. M., Pagel, B. E. J., Edmunds, M. G., & Diaz, A. 1984, *MNRAS*, 210, 701
 Sersic, J. L., & Pastoriza, M. G. 1965, *PASP*, 77, 287
 Syer, D., & Clarke, C. J. 1992, *MNRAS*, 255, 92
 Véron-Cetty, M. P., & Véron, P. 1986, *A&AS*, 66, 335 (VCV)
 Winge, C., et al. 1993, in preparation
 Wolstencroft, R. D., Perley, R., & Tully, R. B. 1984, *MNRAS*, 207, 889
 Wolstencroft, R. D., & Zealey, W. J. 1975, *MNRAS*, 173, 51P
 Zheng, W., Binette, L., & Sulentic, J. W. 1990, *ApJ*, 365, 115
 Zheng, W., Veilleux, S., & Grandi, S. 1991, *ApJ*, 381, 418